

## Heavy meson interquark potential

P. González, V. Mathieu  
and V. Vento

*Departamento de Física Teórica -IFIC  
Universidad de Valencia-CSIC  
E-46100 Burjassot (Valencia), Spain.  
(E-mail: name.surname@uv.es)*

### Abstract

The resolution of Dyson-Schwinger equations leads to the freezing of the QCD running coupling (effective charge) in the infrared, which is best understood as a dynamical generation of a gluon mass function, giving rise to a momentum dependence which is free from infrared divergences. We calculate the interquark static potential for heavy mesons by assuming that it is given by a massive One Gluon Exchange interaction and compare with phenomenological fits inspired by lattice QCD. We apply these potential forms to the description of quarkonia and conclude that, even though some aspects of the confinement mechanism are absent in the Dyson-Schwinger formalism, the spectrum can be reasonably reproduced. We discuss possible explanations for this outcome.

Pacs: 12.38.Gc, 12.38.Lg, 12.39.Pn, 14.40.Pq

Keywords: lattice, meson, quark, gluon, potential

# 1 Introduction

The discovery of asymptotically free constituents of hadronic matter in deep inelastic scattering experiments gave birth to Quantum Chromodynamics (QCD) [1] as the accepted theory of strong interactions. However, the most precise experimental data, the hadron spectrum and hadron properties, have been obtained in the low-energy region. While QCD explains asymptotic freedom [2, 3], it has not been shown to describe confinement of quarks and gluons, nor the realization of chiral symmetry. Therefore, predicting low-energy properties of strongly interacting matter represents a theoretical challenge.

The development of nonperturbative techniques are essential for understanding QCD in this regime. Lattice gauge theory [4, 5] constitutes a nonperturbative regularisation scheme which allows numerical solutions of the theory describing properties of interacting QCD matter [6]. The accuracy of lattice results has been tremendously improved during the past decade with the availability of more powerful computers [7, 8], and lattice results are considered in many instances the data which other nonperturbative schemes should reproduce.

The approximate resolution of the Dyson-Schwinger (DS) equations is another nonperturbative approach which has progressed considerably in the last ten years in great part due to the interplay between their findings and lattice results. It is a more analytical approach and has led to a very appealing physical picture establishing that the QCD running coupling (effective charge) freezes in the deep infrared. This property can be best understood from the point of view of a dynamical gluon mass generation [9, 10].

The aim of this presentation is to investigate the consequences associated to the static interaction one can derive from this picture. For this purpose we calculate numerically the one gluon exchange (OGE) static potential deriving from the DS equations and we compare it to phenomenological potentials whose shape has been inspired by lattice computations. The application of these potentials to the description of quarkonia is discussed.

The paper is written as follows, in the next section we describe some phenomenological potentials justified or motivated by lattice calculations. In Sec. 3 we obtain a potential from the resolution of DS equations and describe some of its characteristics. In Sec. 4 we make a comparative analysis of the different potentials in their application to quarkonia. Finally, in Sec. 5, we summarize our main findings and discuss a possible interpretation of our results.

## 2 Heavy quark dynamics from Lattice

Soon after the discovery of the  $J/\Psi$  mesons in  $e^+e^-$  annihilation, the possibility of a nonrelativistic treatment of such states, in analogy to the positronium of electrodynamics, was suggested [11]. Quarkonia, i.e. mesonic states that contain two heavy constituent quarks, either charm or bottom, owe their name to this analogy.

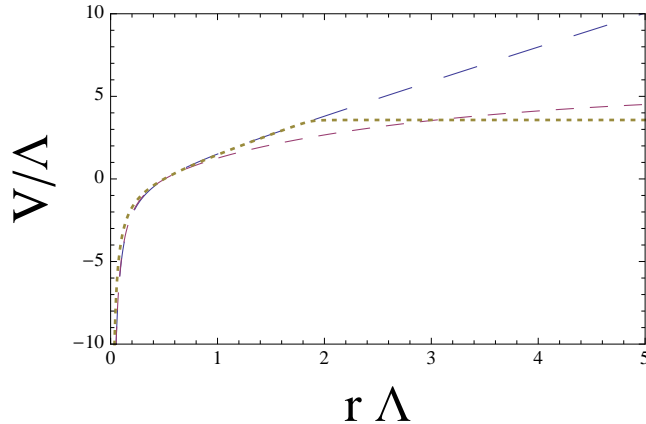


Figure 1: We show the three potentials described in the text : Cornell (solid), Aachen (dashed) and SESAM (dotted). For the Cornell and Aachen potentials the parameters have been chosen phenomenologically to provide a reasonable description of the spectrum and their values are given in Sec. 4. The parameters of the SESAM potential are chosen to reproduce the shape of the Cornell potential at short distances.

For sufficiently heavy quarks, it can be shown in lattice QCD, that the bound state problem becomes essentially nonrelativistic and the dynamics is controlled approximately by a Schrödinger equation with a static potential [12, 13]. Lattice calculations, without dynamical quarks (quenched), give rise to a static potential of the form [12, 13]

$$V(r) = -a/r + br. \quad (1)$$

containing the perturbative expected Coulomb term plus an additional linear term.

The Cornell group, prior to the lattice QCD derivation, using  $a$  and  $b$  as parameters, successfully applied this potential to the phenomenological description of the low lying quarkonia states [14–17] and therefore this potential function is known as the Cornell potential.

Another static interquark potential shape has been guessed by performing unquenched lattice QCD calculations. Using Kogut-Susskind fermions and adopting the lattice spacing from the  $\rho$  mass measurements a potential with the following structure,

$$V(r) = (-\alpha/r + \beta r) \left( \frac{1 - e^{-\gamma r}}{\gamma r} \right), \quad (2)$$

has been shown to describe these lattice results [18]. This parameterization shows screening, associated to quarks loops, which has been cast in the form of the additional factor multiplying the Cornell potential, leading at large values of  $r$  to a constant  $\beta/\gamma$ . Henceforth we shall call this shape the Aachen potential and we shall choose its parameters to provide a reasonable fit to the spectrum.

More recent unquenched lattice calculations have been performed by the SESAM collaboration [19]. The mixing and the transition (string breaking) between  $q\bar{q}$  and  $M\bar{M}$  ( $M$  representing a meson) components have been studied. A correlation matrix for this two-level problem has been considered, the matrix elements incorporating light quark propagators into the standard Wilson loop. Compelling evidence, both for explicit mixing and string breaking, has been demonstrated so that for  $r \geq r_c > 1$  fm ( $r_c$  representing the string breaking distance) the  $M\bar{M}$  configuration becomes energetically favorable. The static  $q\bar{q}$  potential exhibits screening and saturates at twice the mass of the  $M$  meson. An approximate parametrization of it for  $r \leq r_c$  has been proposed,

$$V(r) = m_M + m_{\bar{M}} + g(r)G(r) + C \quad (3)$$

where

$$\begin{aligned} g(r) &= \frac{1}{2} - \frac{1}{\pi} \arctan[d(r - r_c)] \\ G(r) &= -e \left( \frac{1}{r} - \frac{1}{r_c} \right) + \sigma(r - r_c) \end{aligned}$$

with  $C$ ,  $r_c$ ,  $d$ ,  $e$  and  $\sigma$  obtained from lattice results. This parameterization has not the correct long distance limit ( $m_M + m_{\bar{M}}$ ), and differs little from the Cornell potential for  $r < 0.75$  fm.

We show the three potentials in Fig. 1 for comparison<sup>1</sup>. We use in what follows the first two, which contain the two aspects we want to emphasize in here, linear confinement and screening.

### 3 Heavy quark dynamics from Dyson-Schwinger Equations

Infrared finite solutions for the gluon propagator of quenched QCD are obtained from the gauge-invariant nonlinear Dyson-Schwinger equations formulated in the Feynman gauge of the background field method. These solutions may be fitted using a massive propagator [9, 10]. Even though the gluon is massless at the level of the fundamental QCD Lagrangian, and remains massless to all order in perturbation theory, the nonperturbative QCD dynamics generates an effective, momentum-dependent mass, without affecting the local  $SU(3)_c$  invariance, which remains intact.

The gluon mass generation is a purely nonperturbative effect associated with the existence of infrared finite solutions for the gluon propagator,  $\Delta(q^2)$ , i.e. solutions with  $\Delta^{-1}(0) > 0$ . Such solutions may be fitted by a “massive” euclidean propagator of the form [9, 21]

---

<sup>1</sup>The spin-dependent corrections to the potentials above can also be derived from lattice QCD [20]. We do not consider them here.

$$\Delta(q^2) = \frac{1}{q^2 + m^2(q^2)}, \quad (4)$$

where  $m^2(q^2)$  depends nontrivially on the momentum transfer  $q^2$ . One physically motivated possibility, which we shall use in here, is the so called logarithmic mass running, which is defined by

$$m^2(q^2) = m_0^2 \left[ \ln \left( \frac{q^2 + \rho m_0^2}{\Lambda^2} \right) / \ln \left( \frac{\rho m_0^2}{\Lambda^2} \right) \right]^{-1-\delta}, \quad (5)$$

where  $m_0$ ,  $\rho$  and  $\delta$  are parameters whose values are chosen to fit the lattice propagator and  $\Lambda$  is the *QCD* scale. Note that in the limit  $q^2 \rightarrow 0$  one obtains  $m^2(0) = m_0^2$ , giving meaning to  $m_0$ .

Because of the presence of this dynamical gluon mass the strong effective charge extracted from these solutions freezes at a finite value, giving rise to an infrared fixed point for QCD [9, 10]. This nonperturbative generalization of  $\alpha(q^2)$ , the QCD running coupling, comes in the form

$$a(q^2) = \left[ \beta_0 \ln \left( \frac{q^2 + \rho m^2(q^2)}{\Lambda^2} \right) \right]^{-1}, \quad (6)$$

where  $a = \frac{\alpha}{4\pi}$  and we take  $\beta_0 = 11 - 2n_f/3$  where  $n_f$  is the number of flavors. Note that its zero gluon mass limit leads to the LO perturbative coupling constant momentum dependence. The  $m(q^2)$  in the argument of the logarithm tames the Landau pole, and  $a(q^2)$  freezes at a finite value in the IR, namely  $a^{-1}(0) = \beta_0 \ln(\rho m^2(0)/\Lambda^2)$ .

Let us construct a simple potential model where the main source of dynamics is the One Gluon Exchange potential (see Fig. 2) with the propagator and coupling defined by Eqs. 4, 5 and 6.

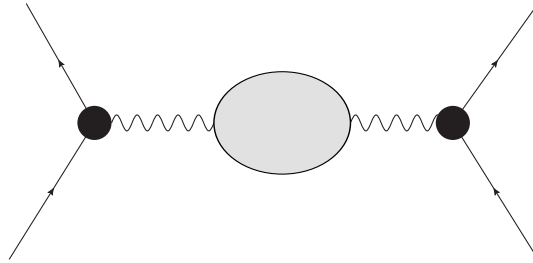


Figure 2: One gluon exchange contribution to the potential.

The potential between static charges is related to the Fourier transform of the time-time component of the full gluon propagator as,

$$V(\mathbf{r}) = -\frac{2C_F}{\pi} \int d^3\mathbf{q} a(q^2) \Delta_{00}(\mathbf{q}) e^{i\mathbf{q}\cdot\mathbf{r}}, \quad (7)$$

where  $C_F$  is the Casimir eigenvalue of the fundamental representation of SU(3) [ $C_F = 4/3$ ], the bold terms,  $\mathbf{q}$  and  $\mathbf{r}$ , are 3-vectors and  $\Delta_{00}(\mathbf{q})$  is the zero-zero component of the gluon propagator in the momentum configuration.

Using the above equations the expression  $a(\mathbf{q}^2) \Delta_{00}(\mathbf{q})$  in the integrand of Eq.7 becomes

$$d(\mathbf{q}^2) = \frac{a(\mathbf{q}^2)}{\mathbf{q}^2 + m^2(\mathbf{q}^2)} \quad (8)$$

with the dynamical mass  $m^2(\mathbf{q}^2)$  and the nonperturbative coupling constant  $a(\mathbf{q}^2)$  defined by Eqs. 5 and 6. This particular combination of propagator and coupling constant is renormalization group invariant. The structure of  $d(\mathbf{q}^2)$  is shown in Fig. 3.

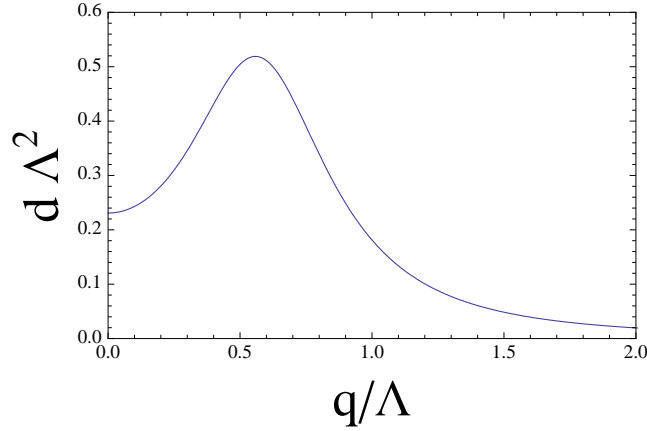


Figure 3: Numerical solution for the RG invariant product  $d$  for  $m_0 = 360$  MeV,  $\rho = 1$ ,  $\Lambda = 300$  MeV and  $n_f = 4$ . We plot the adimensional function  $d\Lambda^2$  as a function of  $\mathbf{q}/\Lambda$ .

In spherical coordinates Eq.7 becomes,

$$V(\mathbf{r}) = -\frac{2 C_F}{\pi} \int_0^{2\pi} d\phi \int_0^\infty d|\mathbf{q}| \mathbf{q}^2 a(\mathbf{q}^2) \Delta(\mathbf{q}^2) \int_{-1}^1 d(\cos \theta) e^{i|\mathbf{q}||\mathbf{r}|\cos \theta}. \quad (9)$$

By performing the angular integral we obtain,

$$V(\mathbf{r}) = -\frac{8 C_F}{|\mathbf{r}|} \int_0^\infty d|\mathbf{q}| |\mathbf{q}| a(\mathbf{q}^2) \Delta(\mathbf{q}^2) \sin(|\mathbf{q}||\mathbf{r}|). \quad (10)$$

The complete QCD potential involves multigluon exchanges, but we assume that the leading nonperturbative term will be sufficient for the description of the spectrum.

In Fig. 4 we show the potential (up to a constant) derived from Eq. 10, i.e. from the DS equations with the definitions in Eqs. 5 and 6. We have chosen the following range of parameters:  $m_0 \sim 360 - 480$  MeV,  $\rho = 1 - 4$ ,  $\delta = 1/11$  [9, 22, 23]. The value of  $\Lambda$  has been taken to be 300 MeV. In order to adjust the behavior at the origin to

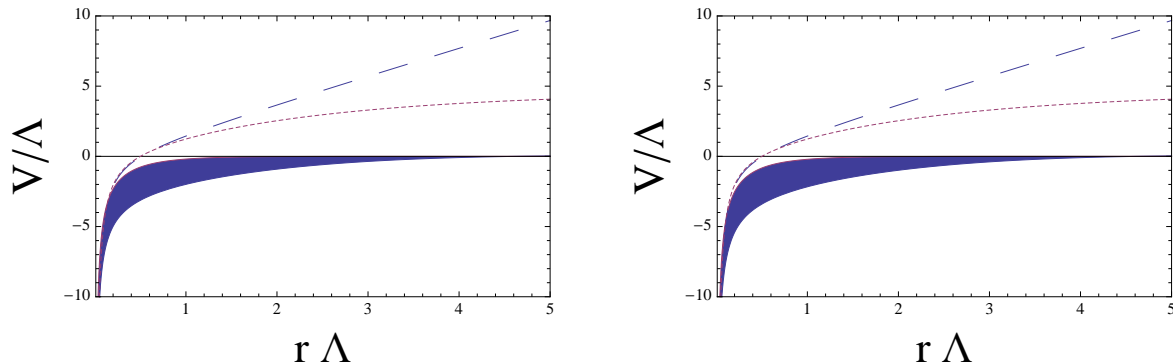


Figure 4: We show the potential obtained from the DS equations. The shaded range corresponds to  $m_0 \sim 360 - 480 \text{ MeV}$  and  $\rho \sim 1 - 4$ . The figure on the left corresponds to 4 flavors ( $\beta_0 = 25/3$ ). The figure on the right corresponds to 5 flavors ( $\beta_0 = 23/3$ ). For comparison we plot the Cornell (dashed) and Aachen (dotted) potentials.

the data we have used  $\beta_0$  corresponding to 4 and 5 flavors. To do this appropriately one should introduce the running of the quark masses, which are at present not well known. However, since asymptotically the masses run to zero, our way of proceeding achieves the correct strength of the potential at low  $r$ . The potential describes well the low radial behavior, by construction, and flattens at large  $r$  going asymptotically to zero.

We should remove from the above calculation the additive infinite self-energy contribution associated with the static sources [12]. In lattice QCD this is done normalizing the potential such that  $V(r_0) = 0$  where  $r_0$  is the Sommer scale [24]. We proceed in the same way but take the subtraction point at the zero of the phenomenological potentials, which happens to be at  $r_0 \sim 0.35 fm$  (see next section). The result of this procedure is shown in Fig. 5. In this way we increase the value of the potential without changing its shape. We call the result of this construction the Dyson-Schwinger (DS) potential. We obtain in this way a potential which resembles the Aachen and not the Cornell potential.

It should be noted that the shape of the DS potential does not vary considerably when we change the parameters within the expected theoretical range. There is no way to reproduce the large  $r$  behavior of the Cornell potential, instead the DS potential flattens and becomes asymptotically constant, similarly to the screened potentials. However, it should not! The approximations used to find the solution to the DS equations do not contain quark loops and therefore they incorporate no mechanism for screening, i.e. a mechanism derivable from the breaking of the string [18, 25]. The truncation in the DS set of equations and the absence of multigluon exchanges might be responsible for the missing linear rise at large  $r$ .

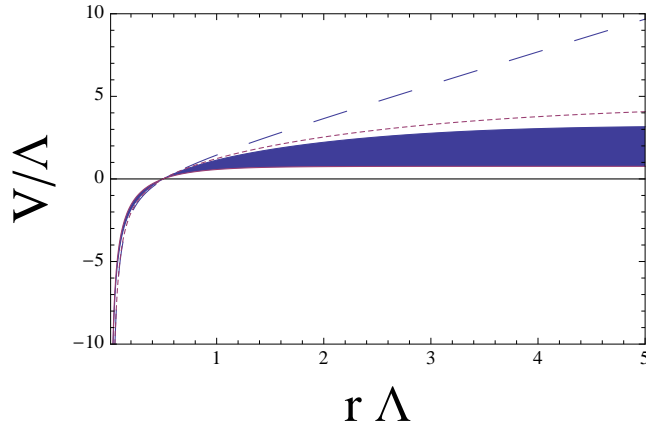


Figure 5: We show the DS potential after the Sommer subtraction, for  $n_f = 4$  and the same range of parameters as in Fig. 4. For comparison we plot the Cornell (dashed) and Aachen (dotted) potentials.

## 4 Quarkonia description by static potentials

The Cornell potential was introduced for phenomenological reasons predating the complete lattice derivation. From the spin-averaged quarkonia spectra it was evident that the underlying potential could not be purely Coulomb type [14]. Therefore, the potential was implemented by a sum of the perturbative expectation plus an additional linear term, recall Eq. 1. Aiming at a universal treatment for charmonium ( $c\bar{c}$ ) and bottomonium ( $b\bar{b}$ ) the Cornell potential has been used with the same values of the parameters,  $a$  and  $b$ , in both cases, for the quark masses,  $m_c$  and  $m_b$ , respectively. A typical range of values providing a reasonable fit to the masses of the low lying states (up to 1.0 GeV excitation energy) is  $a \sim 0.51 - 0.52$  and  $\sqrt{b} \sim 412 - 427$  MeV [15–17]. An example of such spectral fit for charmonium is provided in Table 1 where we have chosen  $\sqrt{b} = 427$  MeV and  $a = 0.52$  with  $m_c = 1350$  MeV and compared the results with masses of experimental resonances having well established  $J^{PC}$  quantum numbers, most of them with  $J^{PC} = 1^{--}$  coming from ISR (Initial State Radiation) processes. The Cornell model provides a good fit to the lower states (at most 30 MeV difference with data) but it cannot accommodate all the known higher energy resonances but only some of them (we use charmonium instead of bottomonium to clarify the effect). For instance  $\psi(4040)$ ,  $\psi(4160)$  and  $\psi(4415)$  maybe assigned to the  $3s$ ,  $2d$  and  $4s$  states respectively. Then other two resonances, cataloged in the Particle Data Group Review [31] as  $X(4260)$  and  $X(4360)$ , cannot be fitted.

The screened potentials introduced initially to fit lattice data have been used phenomenologically [28, 29]. However, the applicability of screened potentials to the spectral description has been a matter of debate [30] since their use is not justified above the meson-meson string breaking threshold. We assume that in the case of quarkonia

$n_r L$	$M_{Cornell}$	$M_{Aachen}$	$M_{PDG}$	$M_{DS}$
	MeV	MeV	MeV	MeV
$1s$	3069	3143	$3096.916 \pm 0.011$	3151
$2s$	3688	3665	$3686.09 \pm 0.04$	3660
$1d$	3806	3775	$3772.92 \pm 0.35$	3761
$3s$	4147	4001	$4039 \pm 1$	4004
$2d$	4228	4072	$4153 \pm 3$	4070
$4s$	4539	4255	$4263^{+8}_{-9}$	4273
$3d$	4601	4306	$4361 \pm 9 \pm 9$	4321
$5s$	4829	4564	$4421 \pm 4$	4487
$4d$	4879	4609		4526
$6s$	5218	4629	$4664 \pm 11 \pm 5$	4651
$5d$	5260	4663		4718
$1p$	3502	3527	$3525.3 \pm 0.2$	3515
$2p$	3983	3894		3886

Table 1: Calculated charmonium masses,  $M_{Cornell}$ ,  $M_{Aachen}$  and  $M_{DS}$  from the Cornell, Aachen and DS potentials. For Cornell and Aachen  $a = \alpha = 0.52$  and  $\sqrt{b} = \sqrt{\beta} = 427$  MeV. The remaining parameter in the Aachen potential has been chosen to be  $\gamma = 0.38$  fm $^{-1}$ . For DS  $\rho = 1$  and  $m_0 = 345.7$  MeV. The charm masses are  $m_c = 1350$  MeV for Cornell and  $m_c = 1400$  MeV for Aachen and DS. Masses for experimental candidates,  $M_{PDG}$ , have been taken from [31]. For  $p$  waves we quote the centroid of the  $np_0$ ,  $np_1$  and  $np_2$  states.

there is an effective string breaking threshold sufficiently high in energy, to allow for a description of the known spectrum in terms of screened potentials. For the sake of comparison the results from the Aachen potential for  $m_c = 1400$  MeV and the same values for the corresponding Cornell parameters  $\alpha = a$ ,  $\beta = b$  are presented in Table 1. The value of  $\gamma = 0.38$  fm $^{-1}$  is fixed to get a reasonable spectral fit. It is important to emphasize that the values of the parameters of the Aachen potential extracted from lattice data [18] can only give a reasonable description of the masses of the low lying quarkonia.

One should keep in mind that these potentials do not contain spin-dependent terms which makes them reliable only when these terms do not play a major role. We use here the conventional approximations, e.g. we consider that these potentials should fit better the spin triplet states and take the centroids of  $p$  states as data for comparison with our results.

The main difference between the Cornell and Aachen potentials refers to the description of the higher excited states. The Aachen potential may allow a one to one assignment of the calculated states to the data.

The similarity of the DS potential (for certain parameter sets) to the Aachen po-

tential as shown in Fig. 5 motivates the exercise of fitting the spectrum with the DS potential. As can be seen in Table 1 this can be achieved for a set of parameters which is close to the expected theoretical range. A low value of the mass,  $m_0 = 345.7$  MeV, is necessary since only with a value close to  $\Lambda$  one gets sufficient strength to achieve, after Sommer subtraction, an asymptotic behavior close to the Aachen potential used in our spectral fit.

Let us discuss the limitations of the parameters used in the fit. The  $\beta_0$  expression is fixed by QCD.  $\beta_0$  is the leading order coefficient of the beta function of the theory, which is scheme independent; the small difference in value implied by the choice of  $n_f$  has almost no effect on the results.  $\Lambda$  is a scale fixed by dimensional transmutation. We take 300 MeV and keep it fixed. The values obtained in experimental fits range from 250 – 300 MeV but we have not even used that liberty. The  $\delta$  value and the variations in the values of  $\rho$  and  $m_0$  are within the limits provided by the DS calculations, in particular  $\Lambda < m_0 < 2\Lambda$  [10,21].

The fit of the spectrum is strongly dependent on the detailed shape of the potential as determined by the mass function and coupling constant, Eqs. 5 and 6 respectively. Recall that the mass function is a fitting function to the lattice results for the propagator [21]. The quality of the spectral fit seems to point out, that the DS potential may qualitatively be a good description of the dynamics.

## 5 Discussion and Conclusions

In order to interpret the above results we have to resort again to lattice calculations. In ref. [26] the authors investigated the origin of the long range linearly rising potential. Using a mechanism described in ref. [27] they were able to subtract the contribution of the center vortices leading to a flat potential as shown in Fig. 6 on the left. On the right of Fig. 6 we show the DS potential after Sommer subtraction and the linear rise of the Cornell potential. It is quite apparent that the figure resembles the one on the left. Therefore we may tentatively conclude that the DS potential contains the physics associated with the approximate gluon interaction but does not contain the physics of the confinement mechanism. We do not advocate any mechanism for confinement in QCD, we only adhere to the fact that the confinement mechanism, whatever it be, is the mechanism behind the rising potential in the quenched approximation.

A surprising result of our calculation is the actual similarity of the DS potential to the Aachen potential as shown in Fig. 5. The latter arises due to the breaking of the string and is represented by a screened potential [18]. The similarity is astonishing more so since we have used conventional values for  $\rho = 1$ ,  $\delta = 1/11$ ,  $\Lambda = 300$  MeV and only varied  $m_0$ , which becomes for the best fit  $m_0 = 345.7$  MeV within the expected range  $\Lambda < m_0 < 2\Lambda$  [10,21].

Not aiming at such precision if we fit the upper extreme of the shaded region, where the DS potential is defined by  $m_0 = 360$  MeV and  $\rho = 1$ , to the Aachen potential shape

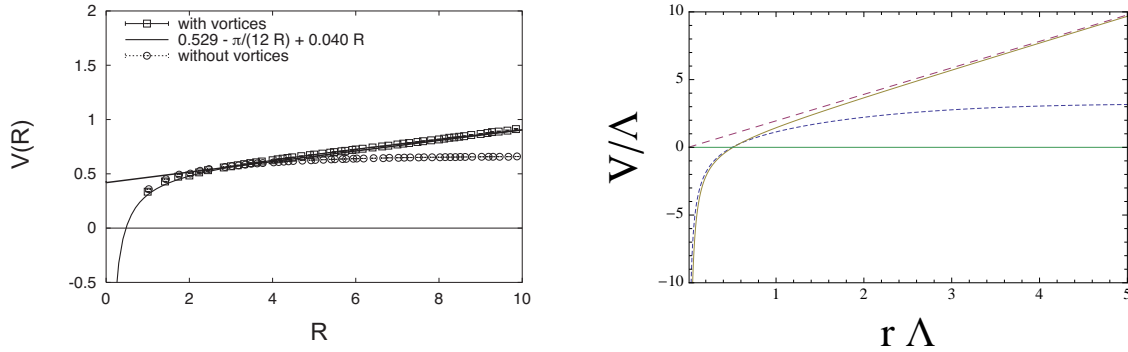


Figure 6: The figure on the left corresponds to the calculation of ref. [26]. In the figure on the right the dotted line corresponds to the DS potential for  $n_f = 4$  and  $m_0 = 360$  MeV and  $\rho = 1$ . The dashed line corresponds to the linear piece of the Cornell potential. The full Cornell potential is drawn (solid line) for comparison.

function we get  $\alpha = 0.40$ ,  $\sqrt{\beta} = 412$  MeV and  $\gamma = 0.53$  fm $^{-1}$ . The other extreme set of parameters for the DS potential, the lower edge of the shaded region,  $m_0 = 480$  MeV and  $\rho = 4$ , leads to  $\alpha = 0.37$ ,  $\sqrt{\beta} = 361$  MeV and  $\gamma = 1.81$  fm $^{-1}$ . It is clear then, that the main difference between the parametrizations arises due to the value of the different screening ranges, which in the Aachen potential is controlled by  $\gamma$ .

Is this similarity accidental or does string breaking imply a dilution of the confinement mechanism associated with multigluon exchanges and/or higher order truncation schemes? Does the Sommer subtraction introduce the energy scale of string breaking? More research needs to be done in order to understand the confinement and string breaking mechanisms though our investigation hints a possible scenario.

In conclusion, we have calculated the OGE potential associated to the approximate resolution of the Dyson-Schwinger equations for the gluon propagator. The low  $r$  behavior is determined perturbatively. The large  $r$  behavior is certainly nonperturbative. The Sommer procedure, to avoid self-energy effects of the static charges, leads to a potential which is not negative at large  $r$ . The approximate resolution of the DS equations is not able to reproduce, at the level of the OGE, the Cornell potential. The DS equations together with the Sommer subtraction is close to the Aachen potential that contains a string breaking mechanism. The fact that we have to push the parameters to the limit of the allowed region to reproduce the spectrum maybe due to the fact that we have not treated the quark mass terms appropriately.

The potential derived from the DS equations might contain most of the dynamics associated with the interquark interaction apart from a non trivial constant which might be related, in the unquenched calculation, to the confinement mechanism.

## Acknowledgement

We would like to thank very instructive conversations with Arlene Aguilar, Daniele Binosi and Joannis Papavassiliou. VV would like to acknowledge clarifying conversations with Stefan Olejnik regarding ref. [26], with Nora Brambilla regarding pNRQCD and the static lattice potential and discussions with Simonetta Liuti about the consequences of our results. We thank the authors of JaxoDraw for making drawing diagrams an easy task [32]. This work has been supported by HadronPhysics2, by MICINN (Spain) grant FPA2010-21750-C02-01, AIC10-D-000598 and by GVPrometeo2009/129. VM has been supported by a post-doctoral grant from CPAN and by a contract from HadronPhysics2.

## References

- [1] H. Fritzsch, M. Gell-Mann and H. Leutwyler, Phys. Lett. B **47** (1973) 365.
- [2] D. J. Gross and F. Wilczek, Phys. Rev. Lett. **30**, 1343 (1973)
- [3] H. D. Politzer, Phys. Rev. Lett. **30**, 1346 (1973).
- [4] K. G. Wilson, Phys. Rev. D **10** (1974) 2445.
- [5] M. Creutz, Phys. Rev. D **21** (1980) 2308.
- [6] M. Creutz, arXiv:1103.3304 [hep-lat].
- [7] C. Sachrajda, PoS **LATTICE2010** (2010) 018 [arXiv:1103.5959 [hep-lat]].
- [8] P. Hagler, Prog. Theor. Phys. Suppl. **187** (2011) 221.
- [9] J. M. Cornwall, Phys. Rev. D **26**, 1453 (1982).
- [10] A. C. Aguilar and J. Papavassiliou, JHEP **0612**, 012 (2006)
- [11] T. Appelquist, H. D. Politzer, Phys. Rev. **D12**, 1404 (1975).
- [12] G. S. Bali, Phys. Rept. **343** (2001) 1-136. [hep-ph/0001312].
- [13] N. Brambilla, A. Pineda, J. Soto and A. Vairo, Rev. Mod. Phys. **77** (2005) 1423 [arXiv:hep-ph/0410047].
- [14] E. Eichten, K. Gottfried, T. Kinoshita, J. B. Kogut, K. D. Lane, T. -M. Yan, Phys. Rev. Lett. **34** (1975) 369-372.
- [15] C. Quigg, J. L. Rosner, Phys. Rept. **56**, 167-235 (1979).

- [16] E. Eichten, K. Gottfried, T. Kinoshita, K. D. Lane, T. -M. Yan, Phys. Rev. **D21** (1980) 203.
- [17] E. Eichten, S. Godfrey, H. Mahlke and J. L. Rosner, Rev. Mod. Phys. **80** (2008) 1161 [arXiv:hep-ph/0701208].
- [18] K. D. Born, E. Laermann, N. Pirch, T. F. Walsh, P. M. Zerwas, Phys. Rev. **D40** (1989) 1653-1663.
- [19] G. S. Bali, H. Neff, T. Duessel, T. Lippert and K. Schilling [SESAM Collaboration], Phys. Rev. D **71** (2005) 114513 [arXiv:hep-lat/0505012].
- [20] Y. Koma and M. Koma, Nucl. Phys. B **769** (2007) 79 [arXiv:hep-lat/0609078].
- [21] A. C. Aguilar, D. Binosi and J. Papavassiliou, Phys. Rev. D **78**, 025010 (2008).
- [22] A. C. Aguilar and J. Papavassiliou, Eur. Phys. J. A **35**, 189 (2008).
- [23] A. C. Aguilar, D. Binosi, J. Papavassiliou and J. Rodriguez-Quintero, Phys. Rev. D **80**, 085018 (2009);
- [24] R. Sommer, Nucl. Phys. B **411** (1994) 839 [arXiv:hep-lat/9310022].
- [25] S. Kratochvila, P. de Forcrand, Nucl. Phys. **B671** (2003) 103-132. [hep-lat/0306011].
- [26] J. Greensite, S. Olejnik, Phys. Rev. **D67** (2003) 094503. [hep-lat/0302018].
- [27] P. de Forcrand, M. D'Elia, Phys. Rev. Lett. **82** (1999) 4582-4585. [hep-lat/9901020].
- [28] Y. B. Ding, K. T. Chao and D. H. Qin, Phys. Rev. D **51** (1995) 5064 [arXiv:hep-ph/9502409].
- [29] P. Gonzalez, A. Valcarce, H. Garcilazo and J. Vijande, Phys. Rev. D **68** (2003) 034007 [arXiv:hep-ph/0307310].
- [30] E. S. Swanson, J. Phys. G **31** (2005) 845 [arXiv:hep-ph/0504097].
- [31] K. Nakamura *et al.* [Particle Data Group], J. Phys. G **37** (2010) 075021.
- [32] D. Binosi, L. Theussl, Comput. Phys. Commun. **161** (2004) 76-86. [hep-ph/0309015].